

THE REDSHIFT OF THE LENSED OBJECT IN THE EINSTEIN RING B0218+357¹

JUDITH G. COHEN,² CHARLES R. LAWRENCE,³ AND ROGER D. BLANDFORD⁴

Received 2002 September 6; accepted 2002 September 23

ABSTRACT

We present a secure redshift of $z = 0.944 \pm 0.002$ for the lensed object in the Einstein ring gravitational lens B0218+357 based on five broad emission lines, in good agreement with our preliminary value announced several years ago based solely on the detection of a single emission line.

Subject headings: galaxies: distances and redshifts — galaxies: individual (B0218+357) — gravitational lensing

1. INTRODUCTION

B0218+357 is a strong flat-spectrum radio source which was discovered to be gravitationally lensed by Patnaik et al. (1993). The object consists of two point sources which are radio loud and variable, with similar flat spectra in the radio regime. In addition to the point sources, there is an Einstein ring of $0''.33$ diameter. This object is the smallest known Einstein radio ring (Patnaik et al. 1993). Biggs et al. (1999) (see also Cohen et al. 2000) have measured a time delay for B0218+357 of 10.5 ± 0.4 days. *Hubble Space Telescope* optical images by Keeton, Kochanek, & Falco (1998) and by Lehar et al. (2000) and NICMOS images by Jackson, Xanthopoulos, & Browne (2000) reveal the lensing galaxy clearly.

B0218+357 is an extremely important object for studies of gravitational lensing. The Einstein ring provides a strong constraint on the mass distribution in the lens. The simple source structure and small angular size of B0218+357, the constraints from substructure in the images which are well mapped with VLBI (see Biggs et al. 2003), and the apparent absence of significant external shear make this object easier than most to model. As the error on the time delay is currently estimated to be 3% (1σ), (A. D. Biggs 2002, private communication), B0218+357 is a prime target for use in determining the Hubble constant and so it is vital to obtain secure and accurate lens and source redshifts.

In order to fulfill the promise of B0218+357 for these purposes, both the source and the lens redshift are required. Browne et al. (1993), and independently Stickel & Kuhr (1993), established the redshift of one of these, which they assumed was the lens, as $z = 0.6847$, detecting several emission and absorption features. Subsequently absorption arising in the lensing galaxy has been detected at 21 cm (Carilli, Rupen, & Yanny 1993), in CO (Wiklind & Coombes 1995), and in formaldehyde (Menton & Reid 1996) against the background source.

However, not surprisingly, the source redshift for B0218+357 proved more elusive, since the source is a blazar

(O’Dea et al. 1992). We therefore started an effort to find the source redshift in 1994 using the Low Resolution Imaging Spectrograph (LRIS) (Oke et al. 1995) at the Keck Observatory. We were able to detect one definite weak emission feature fairly rapidly, but could not find a secure second line. Assuming the detected line at 5460 \AA is the 2800 \AA Mg II line, the redshift of the lensed object in B0218+357 is then $z \sim 0.95$, further supporting Browne et al. (1993), who offer $z = 0.94$ as a “tantalizing possibility, rather than a firm claim.” This result was announced at two conferences in 1996 (Cohen 1996; Lawrence 1996). It has taken longer than expected, but we have finally succeeded in detecting with confidence multiple emission lines from the source. We present in this brief paper the secure redshift of the lensed object in B0218+357 based on the detection of five broad emission lines, $z = 0.944 \pm 0.002$.

2. OBSERVATIONS

In 1994 August, we obtained several exposures with the LRIS of B0218+357, with a total exposure time of 6200 s. The 300 groove mm^{-1} grating was used, and the spectra covered the wavelength region 3000 to 7600 \AA (with no useful signal below 4000 \AA). Figure 1 shows the spectrum of B0218+357 over the central part of this wavelength regime (from spectra with the same instrumental configuration taken in 1997). The steep spectral slope is apparent in this figure. The optical spectrum is fairly red; $F_\nu \propto \nu^\alpha$, with $\alpha \sim -3.5$ (O’Dea et al. 1992). Numerous absorption lines and a few emission lines from the lensing galaxy are clearly seen at the expected redshift, $z = 0.68$ (Browne et al. 1993). In addition, we found a single broad emission line at $\sim 5470 \text{ \AA}$ which has absorption components on its blue wing. We could not find a second emission line within the spectral range covered, and hence the most likely line identification for the detected broad line is Mg II at 2800 \AA , implying z for the lensed object is ~ 0.95 .

If this value is correct, then the next strong emission line to the blue should be C III] 1909 \AA expected to be at $\sim 3720 \text{ \AA}$, while H β should be at about 9500 \AA . Since the blue side of LRIS was not installed until 2001, looking for the C III] line was impossible. Searching for the Balmer lines was also not trivial because these are likely to be weak broad features, and the night sky emission and absorption will create difficulties, but this was judged the only feasible route.

¹ Based on observations obtained at the W.M. Keck Observatory, which is operated jointly by the California Institute of Technology, the University of California, and the National Aeronautics and Space Administration.

² Palomar Observatory, Mail Stop 105-24, California Institute of Technology, Pasadena, CA 91125.

³ California Institute of Technology, Jet Propulsion Laboratory, Mail Stop 169-327, 4800 Oak Grove Drive, Pasadena, CA 91109.

⁴ California Institute of Technology, 130-33, Pasadena, CA 91125.

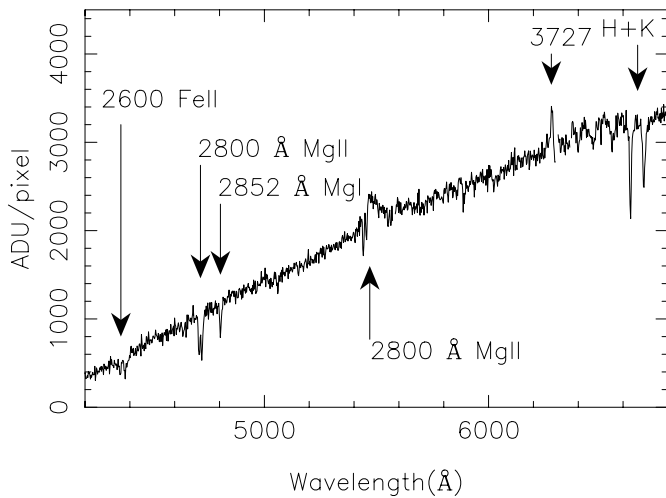


FIG. 1.—Blue spectrum of B0218+357. This is the sum of four 1000 s exposures taken with LRIS in 1997 February. The lines from the lens are labeled above the spectrum, while that from the lensed object (the 2800 Å Mg II line) is labeled below the spectrum. Regions where the night sky emission lines are strong have been omitted.

We took spectra of B0218+357 in the red in 1995, 1996, 1997, and 2000 to hunt for these lines in order to confirm our preliminary redshift. A number of hot stars (white dwarfs or rapidly rotating O stars) selected from Oke (1990) with broad spectral features (and no strong ones within the red region we use here) were observed at similar air mass each night to enable removal of terrestrial atmospheric absorption bands. The object was slightly dithered by several arcseconds along the slit between exposures. The 600 groove mm^{-1} grating blazed at 7500 Å was used, with spectral coverage from 7530 to 10100 Å. A sophisticated reduction and analysis scheme was developed, using the Laplacian cosmic ray removal algorithm of van Dokkum (2001), followed by standard Figaro scripts (Shortridge 1993) for removing distortions in two dimensions, as well as subtraction of the resulting frames. Because both the emission and absorption night sky spectrum are temporally variable (as well as dependent on air mass), this did not result in perfect removal of the night sky emission lines, but it did reduce their intensity by a large factor. This was followed by a removal of the residual night sky emission and, as well as possible, the night sky absorption.

Figure 2 shows the region from 7800 to 8650 Å. The sum of the 1995, 1996, and 1997 red spectra of B0218+357 with a total exposure time of 16,500 s is used. (Several additional spectra of this object taken during that period through thin clouds with lower signal levels were not included.) The summed spectra have been divided by a spectrum of the DAO white dwarf G191-B2B, whose signal level is much higher than that of the spectrum of B0218+357. The spectrum of G191-B2B was normalized to the region near 8800 Å. Prior to this division, the summed, sky-subtracted spectrum of B0218+357 had $\sim 8500 \text{ ADU pixel}^{-1}$ (with $2 e^- \text{ADU}^{-1}$) in the continuum at 8100 Å, and $\sim 2000 \text{ ADU pixel}^{-1}$ in the continuum at 9800 Å. Regions within the strongest night sky lines are omitted in the figure; at such points the curve is discontinuous. This spectral region shows a strong narrow emission line ($\text{H}\beta$ from the lensing galaxy) plus a weaker broad emission line which we interpret as $\text{H}\gamma$ in the background source. The blue wing of the latter is

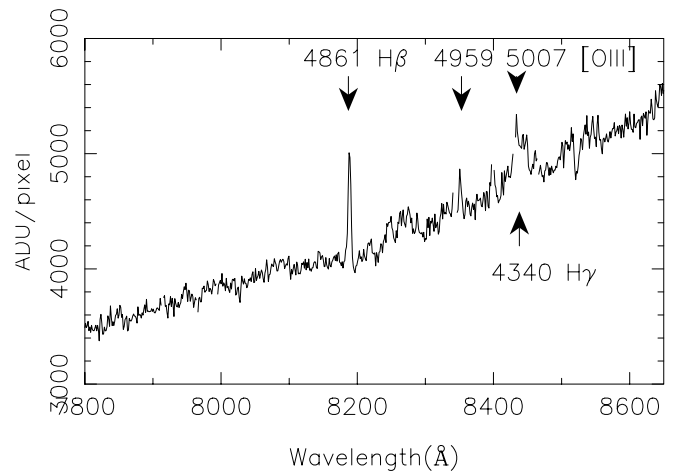


FIG. 2.—Spectrum of B0218+357 from 7800 to 8650 Å. This is the sum of exposures taken with LRIS in 1995, 1996, and 1997 with a total exposure time of 16,500 s. The spectrum has been divided by an exposure of the hot star G191-B2B to remove atmospheric absorption features. As in Fig. 1, the lines from the lens are labeled above the spectrum, while the $\text{H}\gamma$ emission from the lensed object is labeled below the spectrum. Regions where the night sky emission lines are strong have been omitted.

interrupted by the strong 8430 Å night sky emission line. The 4959, 5007 Å [O III] doublet from the lens is present. The bluer line of the doublet is slightly to the red of the strong night sky emission line at 8343 Å (where the curve is discontinuous), while the redder line is mixed in as a sharp peak within the broader $\text{H}\gamma$ from the background source. Small residuals of features from the night sky are also apparent.

The region of $\text{H}\beta$ in the source is shown in Figure 3. Even though this totals to a 16,500 s exposure of B0218+357, the signal is weak due to the decrease in LRIS instrumental efficiency at such red wavelengths. As before, regions where the night sky emission lines are strong have been omitted. The

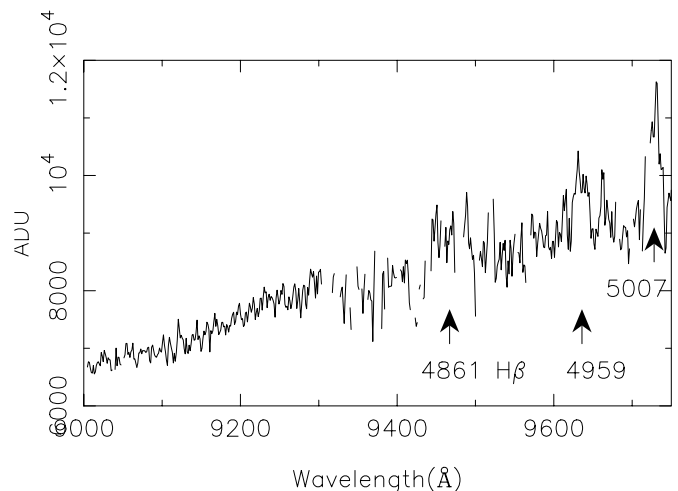


FIG. 3.—Spectrum of B0218+357 from 9000 to 9750 Å. This is a redder section of the same spectrum as shown in Fig. 2. In addition, here the atmospheric absorption bands, which are very strong from 9300 to 9500 Å, were removed by a scaling of the spectra of bright hot stars. Regions where the night sky emission lines are strong or where the hot star spectrum is changing rapidly ($> 8\% \text{ pixel}^{-1}$) have been omitted. The same convention is followed of labeling lines from the lens galaxy above the spectrum and lines from the lensed object below the spectrum.

TABLE 1
FEATURES IN THE SPECTRUM OF B0218+357

Observed λ	Rest λ (\AA)	ID (\AA)	Line Type ^a	Redshift
Lens:				
4357	2586	Fe II	a	0.6848
4378	2599	Fe II	a	0.6845
4709	2797	Mg II (blend)	a	0.6836
4721	2803	Mg II	a	0.6843
4804	2852	Mg I	a	0.6844
6279	3727	[O II] (blend)	e	0.6847
6625	3933.7	Ca II	a	0.6842
6684	3968.5	Ca II	a	0.6843
8188.5.....	4861.3	H β	e	0.6844
8352	4959	[O III]	e	0.6842
8435	5007	[O III]	e	0.6846
9922	5889	Na I	a	0.6846
9933	5895	Na I	a	0.6847
Source:				
5466	2800	Mg II	a	0.952 ^b
8439	4340	H γ	e	0.944
9466	4861	H β	e	0.947
9634	4959	[O III]	e	0.943
9728	5007	[O III]	e	0.943

^a “a” denotes absorption features, and “e” denotes emission lines.

^b Absorption distorts the profile of the blue wing of this line.

spectrum has been divided by an exposure of the hot star G191-B2B to remove atmospheric absorption features normalized as described above. In this spectral region from 9300 to 9500 \AA , the night sky absorption is large and rapidly varying. Regions where the hot star spectrum changed by more than 8 (1 pixel) are also omitted. Furthermore, the absorption in the hot star is slightly scaled to better match the absorption in B0218+357. In addition to H β , the somewhat narrower, but still broad (compared to the lines arising from the lens) lines of the 4959, 5007 \AA [O III] doublet from the source are apparent. Strong, narrow Na D absorption lines from the lens are seen easily in the full spectrum, just redward of the portion shown in Figure 3.

Table 1 summarizes the detected lines from both the source and the lens in B0218+357. Adopting the mean redshift from the four broad emission lines (excluding Mg II 2800 \AA , which is distorted by absorption features), we find $z = 0.944 \pm 0.002$ for the redshift of the lensed object in B0218+357.

2.1. Internal Motions in the Lens

Since the red spectra have higher spectral resolution, we have used the narrow H β emission line in the lens, detected at 8189 \AA , to set an upper limit to the velocity dispersion and/or rotation in the lens galaxy. The instrumental resolution (projection of a 1'' wide slit) of LRIS corresponds at that wavelength to 204 km s^{-1} . We determine an upper limit to the contribution to the FWHM line width from internal motions in the lens galaxy of $\leq 100 \text{ km s}^{-1}$. Pisano et al. (2001) have studied the relationship between the width of H β emission and of 21 cm emission in a sample of galaxies and find that this ratio has a mean of about 0.7, presumably because the ionized gas which gives rise to the former is more centrally concentrated within the gravitational potential of the galaxy.

Our upper limit is consistent with the measured FWHM of the 21 cm absorption line of Carilli, Rupen, & Yanny (1993) of only 43 km s^{-1} . However, the 21 cm absorption presumably probes only a small pencil beam through the lensing galaxy and does not sample its full rotation curve.

The spectral features we detect are consistent with the lens being a spiral galaxy.

3. COMMENT

Given the very heavy use the community has made of our preliminary redshift for B0218+357, published in 1996 (Cohen 1996; Lawrence 1996), it is indeed fortunate that the definitive redshift of $z = 0.944$ presented here confirms our earlier (educated) guess.

The entire Keck/LRIS user community owes a huge debt to Jerry Nelson, Gerry Smith, Bev Oke, and many other people who have worked to make the Keck Telescope and LRIS a reality and to operate and maintain the Keck Observatory. We are grateful to the W. M. Keck Foundation for the vision to fund the construction of the W. M. Keck Observatory. The authors wish to extend special thanks to those of Hawaiian ancestry on whose sacred mountain we are privileged to be guests. Without their generous hospitality, none of the observations presented herein would have been possible. The extragalactic work of J. G. C. is not supported by any federal agency. R. D. B. acknowledges support by the National Science Foundation under grant AST-9900866.

REFERENCES

- Biggs, A. D., Browne, I. W. A., Helbig, P., Koopmans, L. V. E., Wilkinson, P. N., & Perley, R. A. 1999, MNRAS, 304, 349
 Biggs, A. D., Wucknitz, O., Porcas, R. W., Browne, I. W. A., Jackson, N. J., & Wilkinson, P. N. 2003, MNRAS, in press (astro-ph/0209182)
 Browne, I. W. A., Patnaik, A. R., Walsh, D., & Wilkinson, P. N. 1993, MNRAS, 263, L32
 Carilli, C. L., Rupen, M. P., & Yanny, B. 1993, ApJ, 412, L59
 Cohen, A. S., Hewitt, J. N., Moore, C. B., & Haarsma, D. B. 2000, ApJ, 545, 578
 Cohen, J. G. 1996, in ASP Conf. Ser. 88, Clusters, Lensing, and the Future of the Universe, ed. V. Trimble & A. Reisenegger (San Francisco: ASP), 68
 Jackson, N., Xanthopoulos, E., & Browne, I. W. A. 2000, MNRAS, 311, 389
 Keeton, C. R., Kochanek, C. S., & Falco, E. E. 1998, ApJ, 509, 561
 Lawrence, C. R. 1996, in IAU Symp. 173, Astrophysical Implications of Gravitational Lensing, ed. C. S. Kochanek & J. N. Hewitt (Dordrecht: Kluwer), 299
 Lehar, J., et al. 2000, ApJ, 536, 584
 Menton, K. M., & Reid, M. J. 1996, ApJ, 465, L99
 O’Dea, C. P., Baum, S., Stranghellini, C., Dey, A., van Breugel, W., Deustua, S., & Smith, E. P. 1992, AJ, 104, 1320
 Oke, J. B. 1990, AJ, 99, 1621
 Oke, J. B., et al. 1995, PASP, 107, 375
 Patnaik, A. R., Browne, W. A., King, L. J., Muxlow, T. W. B., Walsh, D., & Wilkinson, P. N. 1993, MNRAS, 261, 435
 Pisano, D. J., Kobulnicky, H. A., Guzman, R., Gallego, J., & Bershady, M. J. 2001, AJ, 122, 1194
 Shortridge, K. 1993, in ASP Conf. Ser. 52, Astronomical Data Analysis Software and Systems II, ed. R. J. Hannisch, R. J. V. Brissenden, & J. Barnes (San Francisco: ASP), 219
 Stickel, M., & Kuhr, H. 1993, A&AS, 101, 521
 van Dokkum, P. G. 2001, PASP, 113, 1420
 Wiklind, T., & Coombes, F. 1995, A&A, 299, 382